Hierarchical clustering-based segmentation (HCS) aided interpretation of the DCE MR Images of the Prostate

SELVAN, Arul <http://orcid.org/0000-0001-9222-5538>, PETTITT, Sam and WRIGHT, Chris

Hierarchical Clustering-based Segmentation (HCS) Aided Interpretation of the DCE MR Images of the Prostate

Arul N. Selvan[1]
A.N.Selvan@shu.ac.uk
Sam Pettitt[2]
b2005302@my.shu.ac.uk
Chris Wright[2]
Chris.Wright@shu.ac.uk

[1] Materials and Engineering Research Institute
Sheffield Hallam University,
Sheffield. UK.

[2] Faculty of Health and Wellbeing
Sheffield Hallam University,
Sheffield. UK.

Abstract

In Dynamic Contrast Enhanced Magnetic Resonance Imaging (DCE-MRI) for prostate cancer, there is early intense enhancement and rapid washout of contrast material, due to the heterogeneous and leaky characteristics of the tumour angiogenesis. These characteristics can be demonstrated by the quantitative measurement of signal enhancement with time (Time Intensity Curve). The TIC is plotted for the pixels', averaged intensity value, within a user drawn Region of Interest (ROI). The ROI, normally chosen within an area of the largest enhancement, may enclose tissues of different enhancement pattern. Hence the averaged TIC from the ROI may not represent the actual characteristics of the enclosed tissue of interest.

Hierarchical Clustering-based Segmentation (HCS) is an approach to Computer Aided Monitoring (CAM) that generates a hierarchy of segmentation results to highlight the varied dissimilarities in images. As a diagnostic aid for the analysis of DCE-MR image data, the process starts with the HCS process applied to all the DCE-MR temporal frames of a slice. HCS process output provides heat map images based on the normalised average pixel value of the various dissimilar regions. TIC of the contrast wash-in, wash-out process are then plotted for suspicious regions confirmed by the user. In this paper we have demonstrated how the HCS process as a semi-quantitative analytical tool to analyse the DCE MR images of the Prostate complements the radiologist's interpretation of DCE MR images.

1 Introduction

Dynamic Contrast Enhanced Magnetic Resonance Imaging (DCE-MRI) is useful for evaluating severity, location, and extent of malignancy. However DCE-MRI image interpretation requires substantial experience to accurately detect and categorize lesions.

Hierarchical Clustering-based Segmentation (HCS) [1] implements the traditional bottom-up approach of agglomerative clustering where the regions of an initial partition are iteratively merged [2]. HCS process automatically generates a hierarchy of segmented images by partitioning an image into its constituent regions at hierarchical levels of allowable dissimilarity between its different regions.

doi:30-04-2015#

Tissue abnormality is usually related to a dissimilar part of an image. HCS approach to Computer Aided Monitoring (CAM) [3] generates a hierarchy of segmentation to highlight the dissimilarities allowing the user to derive the maximum benefit from the computational capability (perception) of the machine.

In prostate cancer, the leaky characteristics of the tumour angiogenesis, is demonstrated in DCE-MRI by the early rapid high enhancement just after the administration of contrast medium followed immediately by a relatively rapid decline. In comparison there will be a slower and continuously increasing enhancement for normal tissues [4]. The visual, analysis of DCE-MRI data makes use of the above phenomena. However the visual assessment is inherently subjective.

The above characteristics can also be demonstrated by the quantitative measurement of signal enhancement in DCE-MRI with time. The characteristic shapes of the Time intensity curves (TIC), (Figure 1) may be used for supporting diagnosis. Unlike the visual approach, the semi-quantitative analysis calculates various TIC parameters, sometimes collectively referred to as "curveology." [5]. This approach has been applied successfully in differentiating malignant from normal and pathological but benign prostatic tissue [6][7].

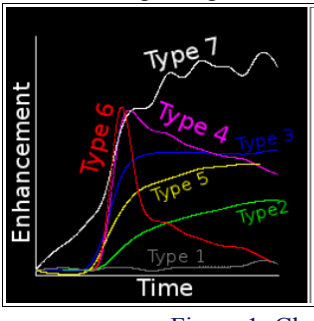

Type 1 (Gray)	: No enhancement; (Benign).
Type 2 (Green)	: Slow enhancement, maximum reached after half scan; (Benign).
Type 3 (Blue)	: Quick enhancement, followed by signal plateau; (Carcinoma).
Type 4 (Magenta)	: Fast enhancement and quick washout; (Carcinoma).
Type 5 (Yellow)	: Quick enhancement, followed by constant enhancement; (Benign).
Type 6 (Red)	: Artery.
Type 7 (White)	: Ambiguous. [Lavini *et al.* 2007]

Figure 1: Classification of Time Intensity Curves (TIC) [8].

2 Materials and Methods

To interpret the DCE-MRI data radiologists select a region of interest (ROI) enclosing a area of the largest enhancement and subsequently observe how the average signal intensity of the voxels within the ROI varies with time (Figure 2A). The ROI, normally chosen within an area of the largest enhancement, because of tissue heterogeneity, may enclose tissues of different enhancement pattern. Hence the averaged TIC from the ROI may not represent the actual characteristics of the lesion. To overcome the approximation, intrinsic to the TIC estimated on pixels averaged within the radiologist drawn ROI, recent studies have proposed to estimate and classify the TIC in every single voxel acquired by the DCE-MRI scan sequence (Figure 2B) [8]. The pixel by pixel analysis of the TIC is sensitive to pixels having different enhancement pattern [9].

The limitations of the pixel by pixel approach is, that it excludes the user from the diagnostic process. Also the resulting classification does not provide any indication how and why pixels are classified as belonging to a specific type. This might lead to the situation where incorrect CAD can have a detrimental effect on human decisions[10][11].

The demonstrated HCS process based TIC classifier method offers the benefits of both the ROI and pixel by pixel approaches by enabling the user to objectively chose a more appropriate ROI and to view a parametric illustration of the TIC (Figure 4). Also the method presents the user with TIC classification of the HCS process's regions (Figure 3).

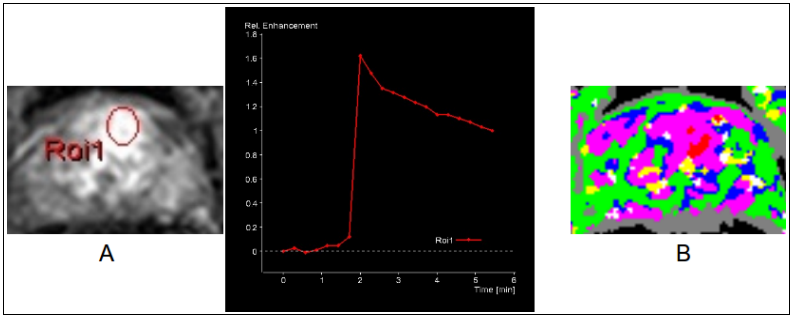

Figure 2: ROI marked by radiologist and its TIC (A), Pixel-by-pixel analysed output (B).

2.1 HCS Process Aided TIC Shape Analysis

The HCS process based TIC shape analysis starts with the HCS process applied to all the DCE-MRI temporal frames of the slice (or the user selected section). The HCS process output provides the heat map images based on the normalised average pixel value of the various dissimilar regions and the regions' boundaries. TICs of the contrast wash-in, wash-out process are then plotted for suspicious regions confirmed by the user (Figures 3 and 4).

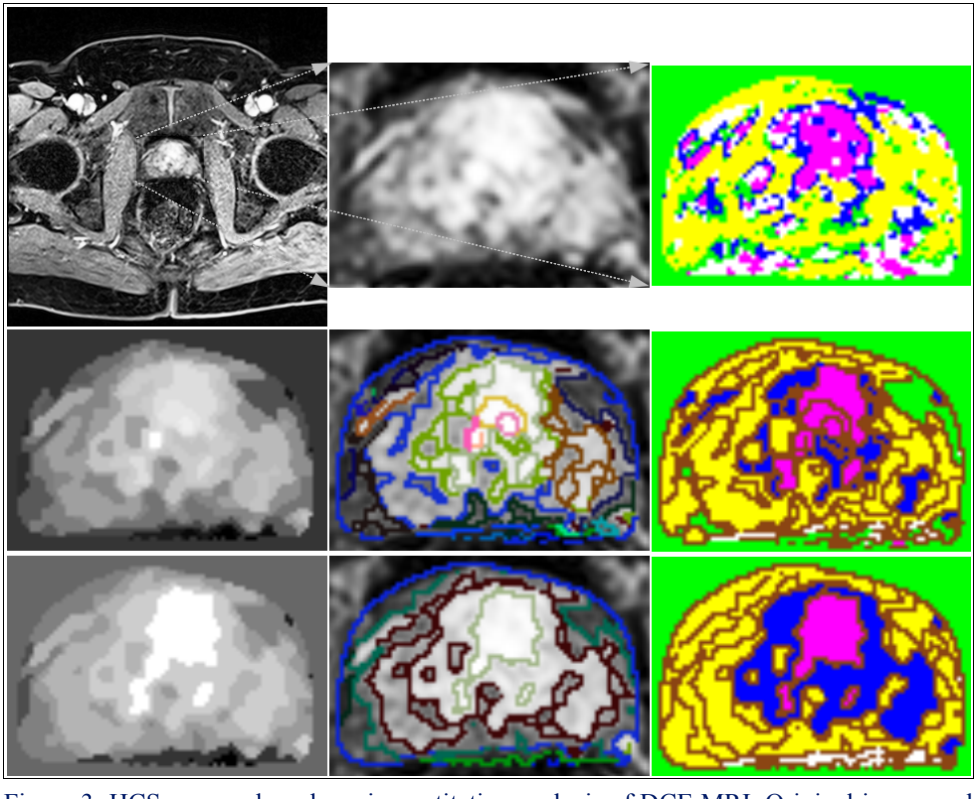

Figure 3: HCS process based semi-quantitative analysis of DCE MRI. Original image and TIC classification at the start of the HCS process (Row 1). Heat map, boundaries and TIC classification of regions for 35 regions (Row 2) and 12 regions (Row 3) of HCS output.

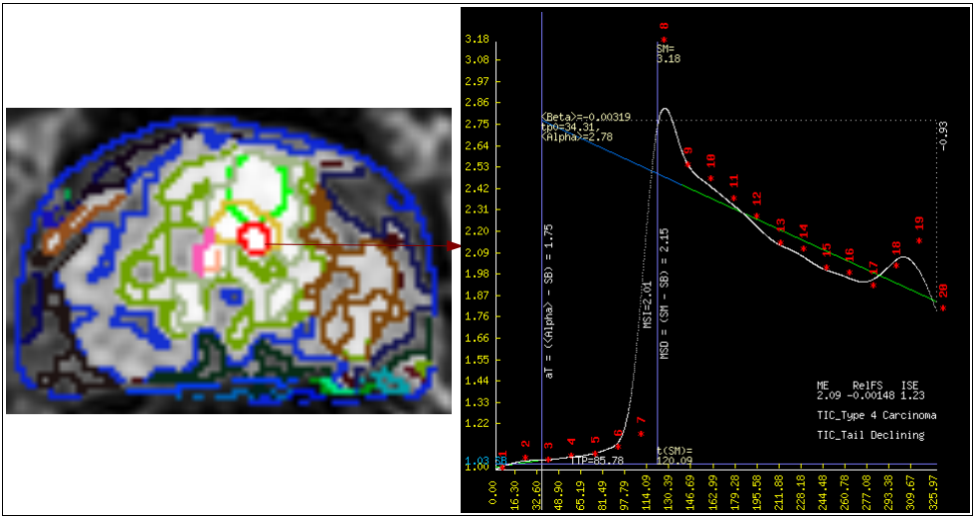

Figure 4: HCS output, and Parametric TIC for user tagged suspicious ROI (Red).

For the TIC shape analysis the signal baseline (SB) was arbitrarily calculated as the average signal intensity of initial three time points before the positive slope occurs (tp = 0). The Tail of the TIC was assumed as the last three quarter of the time points after (tp = 0). The intercept (α) of the line fitted to the tail, with the axis crossing the time axis at the time tp = 0 and the tangent (β) of this line at the last time point was found (Figure 4).

To analyse the shape of the TIC the following features, were used [8]

a) ME :(MSD/SB), where MSD (Maximum signal difference) is the difference between the signal intensity at its maximum S(max) and SB.

b) TTP: Time difference (in seconds) between the moment where the ME occurs and at (tp = 0).For increase-only TICs, the TTP is the last time point in the scan.

c) MSI : Largest positive signal difference between two successive scans.

d) RelFS. : β/MSD. To describe the behaviour of the curves in the last part of the scan: whether it is flat (RelFS = 0), declining (RelFS < 0) or increasing (RelFS > 0).

For the DCE-MRI of the prostate the different TIC types (Figure 1) are classified by a decision tree based on the above features and their threshold values listed in Table 1.

TIC Type	ME	TTP	MSI	RelFS
1	< ME threshold			
2	> ME threshold	> ½ tp(maximum)	< MSD/2.0	> 0.25
3	> ME threshold		> MSD/2.0	-0.25 < RelFS < 0.25 (Flat Tail)
4	> ME threshold	< ½ tp(maximum)	> MSD/4.0	RelFS < -0.25 (Declining Tail)
5	> ME threshold	> ½ tp(maximum)	> MSD/2.0	RelFS > 0.25 (Positive slope Tail)

Table 1 : Threshold values of the features for the classification of the TIC types (Figure 1)

3. Results and Discussion

Anonymised DCE MR image data, in DICOM format, of sixteen cases for which both earlier radiologist's report and the corresponding pathologist's report were available were used for the current study. For each of the sixteen cases the HCS process was applied to the user selected section of interest. The user made use of the HCS process's output of boundary delineated regions and the heat map images based on the normalised average pixel value of the various dissimilar regions to choose the ROI (Figure 3). TIC were plotted for the ROI chosen by the user (Figure 4). Figure 3 also shows the HCS regions coloured as per the TIC types (Figure 1) they were categorised by the HCS process based TIC classification.

For a case to be categorised as abnormal the HCS process based TIC classifier should classify at least one of the regions tagged by the user as carcinoma. For the case to be considered as normal all the regions tagged by the user should be classified as benign.

Table 2 lists the correlation of the radiologist's finding and the HCS process based TIC classification with that of the pathologist's findings. Except for two false positive classification for the rest of the cases the HCS based TIC classifier classification corresponds with the pathology finding. Those two false positive cases have been diagnosed correctly as normal by the radiologist. For those two cases on inspecting the respective TIC the user may discern noisy data (Table 3). It is hypothesised that the HCS based incorrect TIC will not be detrimental for the radiologists.

Radiologist's finding						HCS based TIC classification						Pathology finding Abnormal (A) = 12 Normal (N) = 4
TP	FP	TN	FN	P(TP|A)	P(TN|N)	TP	FP	TN	FN	P(TP|A)	P(TN|N)	
9	1	3	3	75%	75%	12	2	2	0	100%	50%	

Table 2 : Radiologist's finding, HCS process based TIC classification and the Pathology (TP : True Positive, TN : True Negative, FP : False Positive, FN : False Negative)

Case ID	Pathology	TIC Classification	Reason for misclassification
CD1_PAT3	Normal	Carcinoma (False +ve)	Noisy spike in intensity at #8. TTP underestimated (Figure 5)
CD2_PAT6	Normal	Carcinoma (False +ve)	Noisy spike in intensity at #8. TTP underestimated (Figure 5)

Table 3 : Misclassified TIC

4. Conclusion

The demonstrated HCS process based CAM system aids the user to derive the maximum benefit from the computational capability (perception) of the machine and limits the machine's interpretive function. This complementary synthesis of both computer and human strengths enables aids the user to objectively choose the ROI having pixels of similar tissue type, involves the user in the diagnosis process by plotting the TIC for those HCS process segmented regions of interest identified, and the parametric image of the TIC aids the user to visualize the parametric details of the TIC like Time-To-Peak (TTP) and slope of the tail of the TIC. This will aid the user to make a more informed decision to accept or reject the machine's classification which was based on the actual values of those parameters. As a result the HCS based CAM system might improve overall accuracy. For further validation more exhaustive testing of this CAM software is in progress with radiologists and other medical imaging professionals.

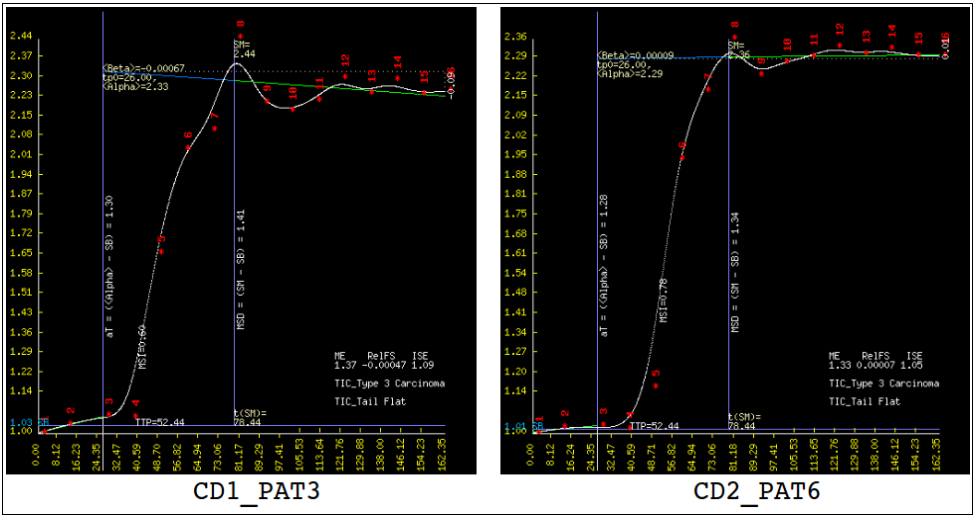

Figure 5: HCS based misclassified TIC.

References

[1] Selvan, A. N. "Boundary Extraction in Images Using Hierarchical Clustering-based Segmentation (HCS)" *BMVC (Student workshop)*, Dundee, UK, Sept 2011.

[2] Nadler, M. and Smith, E. P. "Pattern Recognition Engineering" John Wiley and Sons inc. 1993.

[3] Selvan, A.N.; Saatchi, R. and Ferris, C.M.; "Computer Aided Monitoring of Breast Abnormalities in X-ray Mammograms" *MIUA,* London, UK, 2011.

[4] Engelbrecht MR, *et al.*; "Discrimination of prostate cancer from normal peripheral zone and central gland tissue by using DCE MRI". *Radiology* 2003; 229:248-254.

[5] Verma, S., *et al.* "Overview of Dynamic Contrast-Enhanced MRI in Prostate Cancer Diagnosis and Management" *AJR*:198, June 2012

[6] Noworolski SM, *et al.* "DCE MRI in normal and abnormal prostate tissues as defined by biopsy, MRI, and 3D MRSI". *Magn Reson Med*; 2005; 53:249-255

[7] Jackson AS, Reinsberg SA, Sohaib SA, *et al.*"Dynamic contrast-enhanced MRI for prostate cancer localization". *Br J Radiol*; 2009; 82:148-156

[8] Lavini C., *et al.* "Pixel-by-pixel analysis of DCE MRI curve patterns and an illustration of its application to the imaging of the musculoskeletal system". *MRI*; 2007 June;25(5):604-12.

[9] Lavini, C, Buiter, S. M. and Maas, M. "Use of dynamic contrast enhanced time intensity curve shape analysis in MRI:theory and practice" *Reports in Medical Imaging*. 30 July 2013.

[10] Alberdi, E., *et al.* "Use of computer-aided detection (CAD) tools in screening mammography: a multidisciplinary investigation". *The British Journal of Radiology*; vol. 78, pp. 31-40. 2005.

[11] Fenton, JJ, *et al.* "Effectiveness of computer-aided detection in community mammography practice" *Journal of the National Cancer institute*. 2011 103 (15), 1152-1161.